NUMERICAL SIMULATION OF ATOMIZATION GAS FLOWS

Pedro I. Espina[1], *Stephen D. Ridder*[2], *Ugo Piomelli*[3], *and Francis S. Biancaniello* [2]

Abstract: The gas-flow in a close-coupled gas-metal atomizer was experimentally and numerically studied. Numerically, a method previously employed to model ballistic flows was used to model the atomization gas flows over a range of operational pressures. Experimentally, the jet was examined using schlieren photography searching for the location of predominant flow features. Using these data, the numerical results were validated and a parametric study was conducted to determine the effects of jet pressure ratio on the structure of the gas-only atomization flows. The results obtained explained the observed base-pressure behavior on the basis of the resulting jet structure and flow separation.

Introduction

For the last two decades, the process of gas-metal atomization has gained popularity due to the chemical homogeneity and refined micro-structures exhibited by the powders produced using this technology. However, gas-atomized powders have traditionally been used in high-tech applications where the low yields and high costs of the atomization processing can be justified. Trying to make the process more cost effective, atomization research has focused on the control of the process with aims to increase yields at selected particle sizes.

The control of a molten stream of metal at a temperature near 1700 K[4] is difficult; historically, this has led to atomization control strategies that predominantly focus on the gas-delivery-system of the atomizers. In most atomizers, the gas-delivery-system is an integral part of the *atomization nozzle assembly* – geometrical structure which forces the interaction between a high-speed gas jet and the liquid stream of molten metal. Atomization nozzle assemblies can be of two types: *free-fall*, or *close-coupled*. In free-fall atomizers, the stream of molten metal is allowed to fall unrestricted until it interacts with the gas jet. In close-coupled atomizers, the stream of molten metal is delivered by a ceramic conduit (named *liquid-delivery-tube* or *LDT*) to the interaction zone with the gas jets. Close-coupled atomizers are more difficult to operate, but they tend to produce finer powders than free-fall atomizers. Given that the properties of metal powders generally improve with smaller particle sizes [1], close-coupled atomizers are in high demand and the physics of their gas-only flows (*i.e.,* no liquid metal present) have been the focus of many studies. The reader is referred to reference [2] for a detailed review of gas-only studies of close-coupled gas metal atomizers.

The study here presented makes use of computational fluid dynamics (CFD) to study the gas-only flow produced by a generic close-coupled atomizer. By "generic", it is implied that the geometry of the atomization nozzle assembly was selected to be representative of numerous designs used by other researchers and industry. The operational parameters are based on those typically used for the production of metal powder [3].

Both experimental and numerical results are presented. Experimentally, the atomization gas-only flow is examined using schlieren photography to identify the position of prominent flow features. These data are used to validate the CFD results over a wide range of conditions. A parametric study is conducted to determine the effects of jet pressure ratio on the structure of the gas-only flows and to explain the observed base-pressure at the end of the LDT (*i.e.,* aspiration pressure).

[1] Mech. Eng., National Institute of Standards and Technology (NIST), Bldg. 230, Rm. 105, Gaithersburg, MD 20899.
[2] Metallurgist, NIST, Bldg. 231, Rm. B156, Gaithersburg, MD 20899.
[3] Assoc. Prof., Dept. of Mech. Eng., Univ. of Maryland, College Park, MD 20742.
[4] Typical temperature of Ni based superalloys during atomization.

Numerical Method

The axisymmetric, steady, compressible flow in an atomizer is governed by the non-reacting Navier-Stokes equations. In this work, the solution to the Navier-Stokes equations was accomplished using the NPARC code [4] while the solution to the turbulence equations was obtained using a compressible implementation of Chien's k-ϵ model [5]. However, in this investigation, the production of turbulence kinetic energy dissipation in the k-ϵ model was reduced 10% to correct for its over-prediction in this type of jet as suggested in reference [6].

The computational domain used in this investigation (Figure 1) is an annular jet implementation of the close-coupled atomizer used in reference [3]. The computational domain was segmented into three separate blocks: *Block 1* – annular channel (discretized using 42×41 points in the axial and radial directions respectively), *Block 2* – volume over the LDT (57×161), and *Block 3* – volume after the axial-end of the LDT (289×215). Blocks 2 and 3 extend radially to a distance of $10R$, while block 3 extends axially to a distance of $14.7R$ from the exit-plane of the annular channel. Within each block, the mesh points were distributed using the SAGE grid adaptation program [7]. Complete details regarding the various aspects of the numerical method here used can be found in references [6, 8].

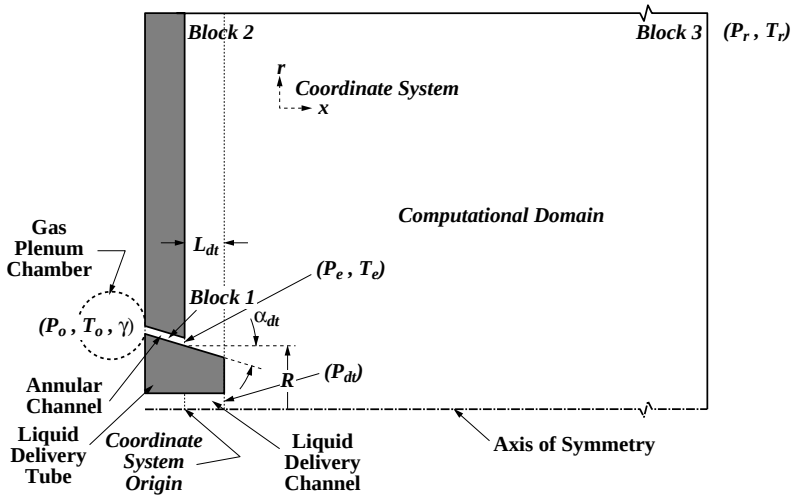

Figure 1: Schematic diagram of the computational domain used to model the gas-only flow in a close-coupled atomizer.

Results

Some of the parameters controlling the performance of close-coupled atomizers are typically fixed by the design (*e.g.,* R and α_{dt} in Figure 1). Others can be changed prior to the initiation of the atomization process (*e.g.,* L_{dt} and the gas specie). However, a number of parameters can be changed *in situ*, providing the ability to modify the atomization process output based on some product quality measurement (*e.g.,* P_r, P_e, T_r, and T_e). In this work, we study the combined effect of both jet pressure, P_e, and receiving chamber pressure, P_r, on the structure of the gas-only flow produced by the atomization geometry shown in Figure 1. This combined effect is captured as a function of the dimensionless jet pressure ratio, $P_e/P_r = P_o/P_r \left(\frac{\gamma+1}{2}\right)^{\frac{\gamma}{1-\gamma}}$, in the results that follow.

– **Effects of Jet Pressure Ratio:** To investigate the effects of the dimensionless jet pressure ratio we chose to model five jets at pressure ratios of $P_e/P_r = 6.6$, 20, 33, 46, and 53 (although only the results for the lower four pressure ratio jets are discussed in detail due to the similarities between the $P_e/P_r = 46$ and 53 jets). Numerical density contours are compared to experimental schlieren images in Figure 2. Overall, good agreement can be observed between experimental data and numerical results; the flow structures (shock

waves, expansion fans, shear layers) observed in the experiments are also present in the calculations, and their locations are generally correct.

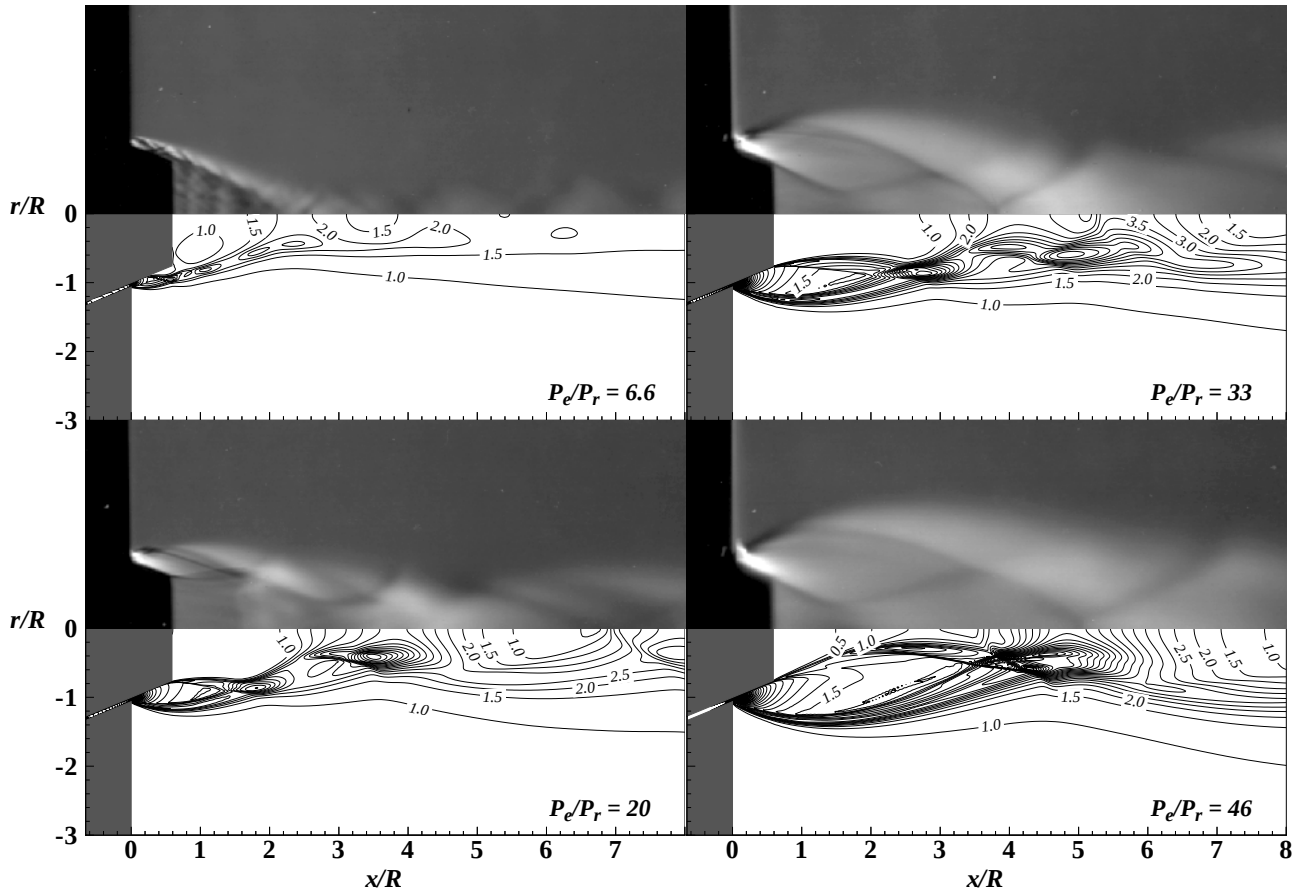

Figure 2: Effect of jet pressure ratio on the structure of gas-only atomization flows: experimental schlieren pictures (upper images), numerical density distribution, $\rho^* = \rho/\rho_r$ (lower images): $\Delta\rho^* = 0.5$.

Regardless of pressure, a significant number of features in these close-coupled atomization gas-only flows remain unchanged. Initially, as the gas exits the plenum chamber (see Figure 1), it accelerates from a quasi-stagnated state to sonic conditions (*i.e.,* Mach Number = 1) along the length of the annular channel. At the exit of the channel, the flow emerges with a pressure higher than the receiving-chamber pressure and forms an underexpanded wall-jet over the outer surface of the LDT (see Figure 2). For most pressure ratios of interest to atomization, this wall-jet separates somewhere along the surface of the LDT forming an annular underexpanded jet that entraps a volume of fluid at the base of the LDT. The resulting base flow has characteristics similar to those seen in other axisymmetric supersonic base flows [6], and its structure has a direct influence on the pressure sensed at the base of the LDT (*i.e.,* aspiration pressure). At the end of the separation region, the jet flow looses its annular character and becomes a single supersonic jet. Thereafter, the jet continues downstream through a series of barrel-shocks[(5)] until it looses enough momentum to become subsonic.

The most predominant change associated with a variation in jet pressure ratio is the variation in size and shape of the separation region at the base of the LDT. At low pressure ratios, $P_e/P_r \simeq 6.6$ (top image in Figure 2), the annular flow encapsulates a conically shaped region at the base of the LDT which is relatively short ($x/R < 2.05$). For $P_e/P_r \simeq 20$ (second image from the top in Figure 2), the middle

[(5)] A "barrel-shock" is a repetitive barrel-shaped flow structure initiated by an expansion fan and terminated by an oblique shock wave. The resulting flow pattern is often seen in supersonic jets as a series of diamonds.

portion of the initial barrel-shock in the annular jet pinches the separation streamline, giving the separation region a longer ($x/R < 2.80$) hourglass shaped form. At $P_e/P_r \simeq 33$ (third image from the top in Figure 2), the previous trend is accentuated as the middle portion of the initial barrel-shock further pinches the center of the separation bubble, leading to a longer ($x/R < 3.65$) and narrower separation region than those seen before. However, with further increases in jet pressure ratio, $P_e/P_r > 33$ (bottom image in Figure 2), the initial barrel-shock in the flow grows to a size which forces the inner shear-layer very close to the axis of symmetry at an early stage along the path of the jet. This, in turn, renders short, conically shaped separation regions ($x/R < 2$), with encapsulated flows that lead to significantly different aspiration pressure behavior from that seen at lower pressure ratios.

Figure 3 shows experimental and numerical results for the aspiration pressure as a function of the jet pressure ratio. The experimental results, which are typical of this type of atomizer [3], have uncertainties no larger than the size of the symbols used in the plot. In general, the numerical calculations miss the prediction of the aspiration pressure by 10-20% (a result consistent with similar numerical data obtained from supersonic base flow simulations [6]). However, the simulations capture accurately the trends observed in the experimental data thus enabling the correlation of the flow field structure with the observed aspiration behavior.

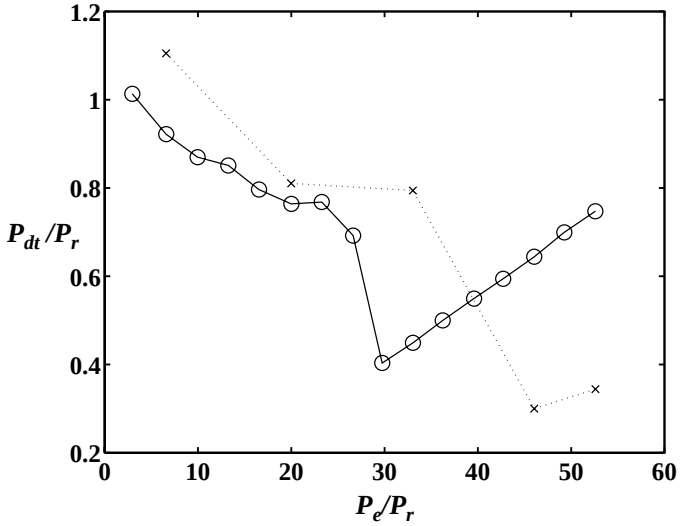

Figure 3: Effect of jet pressure ratio, P_e/P_r, on aspiration pressure, P_{dt}/P_r, for the selected atomization geometry. —○— : experimental data, $P_{r_{exp}} = 98.574\ kPa$; —×— : numerical results.

At low pressure ratios, $P_e/P_r < 5$, as seen in the experimental data, the LDT experiences a high aspiration pressure, $P_{dt}/P_r > 1$, that can lead to a "blow-back" condition (*i.e.,* gas flowing into the LDT and bubbling through the liquid metal in the crucible, generally leading to a freeze-off). For mid-range pressure ratios, $5 < P_e/P_r < 25$, the LDT records ever decreasing aspiration pressures that plateau near $P_e/P_r \simeq 20$. For a narrow range of pressure ratios thereafter, $25 < P_e/P_r < 30$, the aspiration pressure decreases rapidly, leading to its minimum value, or *maximum aspiration condition.* Further increases in jet pressure ratio lead to linear increases in aspiration pressure, eventually leading to a second blow-back regime.

– **Flow Separation and "Freeze-Off":** An important feature of these jets is the flow separation that may occur over the outer surface of the LDT for some conditions (see Figure 4). The occurrence of separation, which is a function of jet pressure ratio and LDT extension, has been suggested [9] to cause liquid metal to be drawn from the end-face of the LDT into its outer surface, where it is exposed to the very cold expanding gas of the annular wall-jet. The extreme temperature difference between the metal and the gas promotes the solidification and accumulation of metal, leading to a shape alteration of the LDT. Typically, this sequence of events induces a freeze-off that ends the atomization process prematurely.

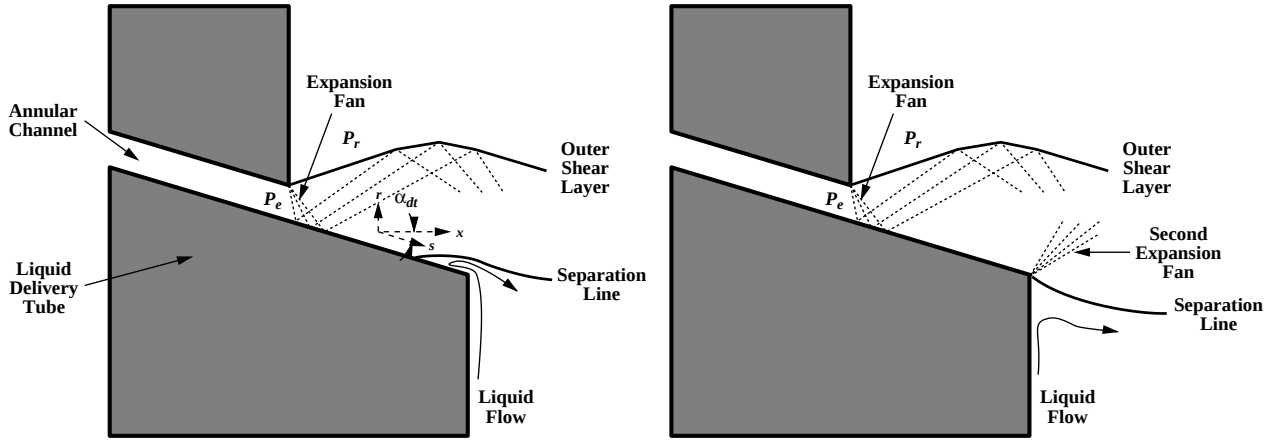

Figure 4: Schematic diagram of the flow separation phenomenon at the end of the LDT. LEFT: early separation at low values of P_e/P_r; RIGHT: secondary expansion process at high values of P_e/P_r.

Figure 5 shows the skin friction coefficient, C_f,[6] over the surface of the LDT as a function of surface distance, $s = x/cos(\alpha_{dt})$, for four pressure ratios. At all pressure ratios, the friction coefficient increases early in the length of the LDT due to the flow acceleration caused by the expansion fan emanating from the end-lip of the annular channel (see Figure 4). From there on, the friction coefficient decays smoothly as the wall-jet boundary layer looses momentum to friction. For pressure ratios, P_e/P_r, lower than 33, the simulations predict that the flow will separate before it reaches the end of the LDT. However, at the high pressure ratios ($P_e/P_r \simeq 46$), the flow never separates before the end of the LDT.

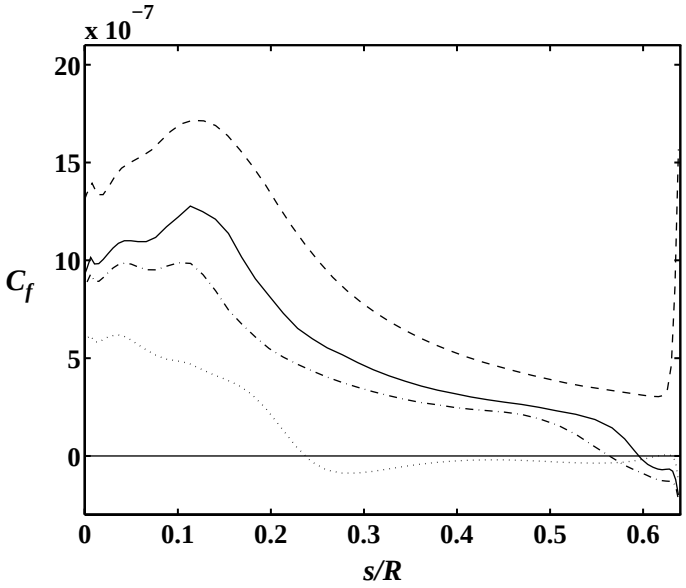

Figure 5: Effect of jet pressure ratio on flow separation over the LDT : $C_f = 2\,\tau_w/\rho_r a_r^2$. ·····: $P_e/P_r \simeq 6.6$; -·-·-: $P_e/P_r \simeq 20$; ——: $P_e/P_r \simeq 33$; - - -: $P_e/P_r \simeq 46$.

The observed behavior leads to the following model of the aspiration phenomenon that describes the trend experimentally, shown in Figure 3. For mid-range pressure ratios, $P_e/P_r < 20$ (decreasing P_{dt}/P_r range), the flow over the LDT separates early on along its trajectory over the LDT. In this range, the

[6] Ratio of the shear stress imposed by the flow on the wall to the flow inertial forces. $C_f = 0$ denotes the point where the flow separates from the wall.

decrease in aspiration pressure with increasing pressure ratio results from an ever larger expansion level due to the increasing underexpansion of the wall-jet (*i.e.,* as the pressure ratio increases the separation point moves downstream allowing for more expansion in the wall-jet and thus, lower pressures in the flow encapsulating the base region). At pressure ratios between 20 and 25 (plateau in P_{dt}/P_r range), the flow separates close to the end of the LDT, leading to an aspiration pressure level that is controlled by the dynamics of the flow in the hourglass shaped separation bubble. Given that the structure of the hourglass shaped separation bubble does not change significantly in this pressure ratio range, then it follows that the aspiration pressure remains fairly constant. For higher pressure ratios, $P_e/P_r > 25$ (increasing P_{dt}/P_r range), the flow never separates from the face of the LDT and a second expansion fan forms at its end-corner. This second expansion controls both the shape of the separation region and the aspiration pressure. As pressure ratio increases, so will the pressure upstream of the second expansion process. Given the aerodynamic conditions present, the second expansion process will yield ever smaller separation regions with ever increasing aspiration pressures.

Conclusions

The gas-only flow fields in close-coupled gas-metal atomizers were computed using methodologies previously tested in similar configurations [6]. Simulations were carried out to determine the effect of jet pressure ratio on the gas-only atomization flow. Five jet pressure ratios were considered, P_e/P_r = 6.6, 20, 33, 46, 53. The numerical results showed that, although the aspiration pressure was not predicted with satisfactory accuracy, the resulting jet structure was in good qualitative agreement with experimental schlieren pictures. The wall-jet flowing over the LDT separated for a certain set of conditions leading to a possible freeze-off condition. Given the severe consequence of flow separation over the LDT for the atomization process, it is advisable to make use of short LDTs to avoid flow separation. The separation behavior seen, in conjunction with the observed jet structure, lead to a phenomenological model which describes the aspiration behavior observed experimentally. Our results suggest that the operation of the atomizer in the increasing P_{dt}/P_r range reduces the chances of separation at the end of the LDT, thus avoiding the possibility of a freeze-off.

References

[1] Boettinger, W. J., Bendersky, L., & Early, J. G. 1986 An Analysis of the Microstructure of Rapidly Solidified Al-8 Wt. Pct. Fe Powder. *Met. Trans. A*, **17** (1), 781–790.

[2] Espina, P. I., & Piomelli, U. 1998 Numerical Simulation of the Gas Flow in Gas-Metal Atomizers. *Proceedings of the 1998 ASME Fluids Engineering Division Summer Meeting* (Washington, DC: ASME 1998), FEDSM98-4901.

[3] Ridder, S. D., & Biancaniello, F. S. 1988 Process Control During High Pressure Atomization. *Mat. Sci. Eng.*, **98**, 47–51.

[4] Cooper, G. K., & Sirbaugh, J. R. 1989 PARC Code: Theory and Usage. AEDC–TR–89–15, Arnold Engineering Development Center, Arnold AFB, TN.

[5] Georgiadis, N. J., Chitsomboon, T., & Zhu, J. 1994 Modification of the Two-Equation Turbulence Model on NPARC to a Chien Low Reynolds Number k-ϵ Formulation. NASA TM–106710.

[6] Espina, P. I., & Piomelli, U. 1997 A Validation of the NPARC Code in Supersonic Base Flows. AIAA Paper 97–0032.

[7] Davies, C. B. & Venkatapathy, E. 1992 Application of a Solution Adaptive Grid Scheme to Complex Three-Dimensional Flows. *AIAA J.*, **30** (9), 2227–2233.

[8] Espina, P. I., & Piomelli, U. 1998 Study of the Gas Jet in a Close-Coupled Gas-Metal Atomizer. AIAA Paper 98–0959.

[9] Ridder, S. D., Osella, S. A., Espina, P. I., & Biancaniello, F. S. 1992 Intelligent Control of Particle Size Distribution During Gas Atomization. *Int. J. of Powder Met.*, **28** (2), 133–138.